VOL. 20, NO. 21, NOVEMBER 2025 ISSN 1819-6608
ARPN Journal of Engineering and Applied Sciences

www.arpnjournals.com

SLOTTED GROUND PLANE TECHNIQUE FOR MUTUAL COUPLING REDUCTION OF CLOSELY MIMO OF PIFA ELEMENTS

Malik Jasim Hussein[1,2], Wa'il A. Godaymi Al-Tumah[1] and Ahmad H. AL-Shaheen[3]
[1]Department of Physics, College of Science, University of Basrah, Iraq
[2]Muthanna Education General Management, Iraq
[3]Department of Physics, College of Science, University of Misan, Iraq
E-Mail: wail.godaymi@uobasrah.edu.iq

ABSTRACT

This work presents the design of a compact two-element semicircular PIFA MIMO antenna employing a slotted ground plane to reduce mutual coupling. The concept is to introduce simple rectangular slots at the centre of the ground plane, which markedly improve isolation while keeping the antenna footprint compact. Simulation results show a strong reduction in coupling, with S21 enhanced from -19.46 dB to -40.71 dB at 5.75 GHz, together with a wider impedance bandwidth that supports modern wireless applications. Fabricated prototypes validated the design, achieving a measured isolation of -35.4 dB. Key diversity metrics were also examined, including Envelope Correlation Coefficient (ECC), Diversity Gain (DG), Channel Capacity Loss (CCL), Mean Effective Gain (MEG), and Total Active Reflection Coefficient (TARC). The results confirm excellent diversity performance. Overall, the proposed structure offers a practical and low-cost solution for compact devices requiring improved MIMO performance in 5G, Wi-Fi, and IoT systems.

Keywords: planar inverted-f antenna (PIFA), HFSS, mobile communication, multiple-input–multiple-output (MIMO) systems.

Manuscript Received 13 October 2025; Revised 15 January 2026; Published 25 January 2026

1. INTRODUCTION

Mobile telecommunication devices were originally intended solely for voice communication. With the rapid evolution of wireless technologies and mobile communication systems over the past two decades, however, mobile terminals have undergone a significant transformation, resulting in a dramatic rise in both functionality and market penetration. As user demand for high-speed data services has grown, the challenge of achieving the required data rates within limited spectral resources has become increasingly critical. A breakthrough in addressing this limitation was the introduction of Multiple-Input Multiple-Output (MIMO) technology, which leverages multiple antennas at both the transmitting and receiving ends to improve channel capacity without requiring additional bandwidth [1-5].

The foundations of MIMO were laid by Winters in 1987, when the principle of employing multiple antennas for enhanced channel throughput was first proposed [6]. By the late 1990s, MIMO had gained recognition as a practical and highly effective method for increasing spectral efficiency [7, 8]. Comparative studies consistently demonstrated that MIMO systems provide far greater capacity improvements than conventional Single-Input Single-Output (SISO) systems, thereby establishing MIMO as a cornerstone of modern wireless communication [8].

Despite its well-documented benefits, the application of MIMO technology to compact wireless terminals poses substantial challenges. One of the most significant limitations arises from the strong electromagnetic interaction between closely spaced antenna elements, known as mutual coupling. This phenomenon alters the input impedance of the radiating elements and distorts their radiation characteristics [9]. Empirical studies have shown that strong mutual coupling increases the envelope correlation between antenna ports, leading to significant degradation in channel capacity [10-13].

Theoretically, mutual coupling can be minimized when antenna elements are placed at distances greater than half a wavelength [9]. However, this requirement is rarely feasible in compact devices such as smartphones, where physical constraints impose strict limitations on antenna spacing. Consequently, MIMO systems have been more easily deployed in infrastructures such as base stations and wireless access points, where large antenna arrays can be accommodated. The integration of MIMO into handheld devices, therefore, remains a persistent design challenge, motivating extensive research into strategies that can effectively reduce coupling while preserving compactness. Several techniques have been proposed to improve isolation between antenna elements in small-form-factor devices. Among them, innovative antenna geometries and the incorporation of Electromagnetic Band-Gap (EBG) structures have been widely investigated for their ability to suppress surface-wave propagation and improve port isolation [14-21]. In parallel, defective ground plane approaches, such as the introduction of slots and slits, have attracted attention due to their simplicity, low cost, and compatibility with conventional printed circuit board fabrication [22-25].

In light of these challenges, a novel two-element semicircular Planar Inverted-F Antenna (PIFA) MIMO design is proposed in this dissertation. The configuration incorporates a pair of precisely engineered slots in the ground plane, which act to suppress surface currents and thereby mitigate mutual coupling. Through this design,

superior isolation and improved diversity performance are achieved compared with conventional PIFA arrays, making the proposed antenna a strong candidate for next-generation compact wireless devices operating in the C-band.

2. GEOMETRY OF ANTENNA

The geometrical top view, back view, and side view of the proposed patch antenna are shown in Figure-1, respectively. A semicircular antenna was designed to operate at a frequency of 5.8 GHz. The ground plane dimensions are 16 mm by 19 mm. The patch antenna is fabricated on the two-layer insulating substrates, the lower one is a FR4-Epoxy substrate with a thickness (h_1) of 1.6 mm, relative permittivity (ε_r) of 4.4, and loss tangent (tan δ) of 0.02, and the second is air, with a height (h_2) of 2 mm. The equivalent relative dielectric constant of 1.52 was calculated using the equation [9][26]:

$$\varepsilon_{eqr} = \frac{\varepsilon_{r1}\varepsilon_{r2}(h_1+h_2)}{\varepsilon_{r1}h_2+\varepsilon_{r2}h_1} \quad \ldots\ldots\ldots\ldots\ldots\ldots\ldots 1$$

The antenna radius was calculated using equation:

$$r = 0.005\left(\frac{4}{\pi}\left(\frac{c}{4f_r\sqrt{\frac{\epsilon_{r+1}}{2}}} - H\right)\right)^2 + 0.57\left(\frac{4}{\pi}\left(\frac{c}{4f_r\sqrt{\frac{\epsilon_{r+1}}{2}}} - H\right)\right) + 2.3 \quad \ldots\ldots\ldots\ldots\ldots\ldots 2$$

which was found is about 9 mm, therefore the shorting strip width is 18mm. A probe feed technique with an input impedance of 50 Ω was used the feed location is (0.8mm). High Frequency Structure Simulation (HFSS) is used as a tool to carry out the analysis and enhance the performance of the suggested antenna.

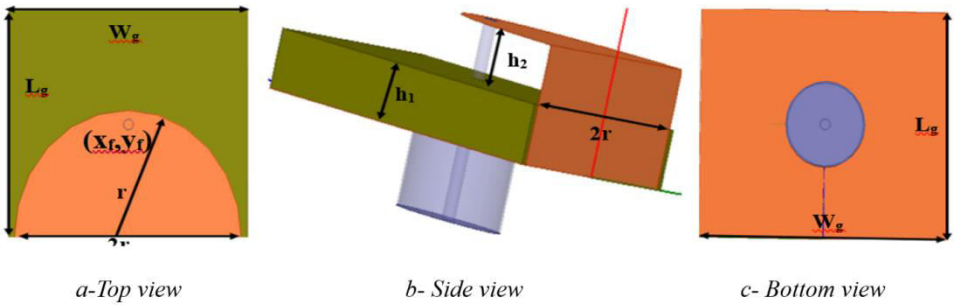

Figure-1. Proposed PIFA (a) Top view, (b) Side view, and (c) Back side.

3. RESULTS AND DISCUSSIONS

This section examines the performance of the proposed antenna, focusing on its radiation pattern, beamwidth, and return loss. The antenna design and simulations were carried out using HFSS software. Figure-1 presents the simulation results for return loss and 3D total gain, showing a minimum return loss of -51.91 dB at 5.84GHz with a bandwidth of 17.38%and a maximum gain of 4.13 dB, while Figure-2 illustrates the input impedance and VSWR, where the impedance was measured at 49.9 Ω, and the VSWR was 1.005. Additionally, as seen from the simulation results, the parameters are calculated for the radius, and the feed location is good according to the value of S_{11}, input impedance, and VSWR. Figure-3 depicts the radiation pattern's directivity and gain in both the E and H planes, with the highest directivity recorded at 5.8 GHz is 4.2dB. To examine the radiation efficiency, the gain and directivity are plotted for 5.8 GHz; the efficiency was found 98% for both E and H planes, as shown in Figure 4.

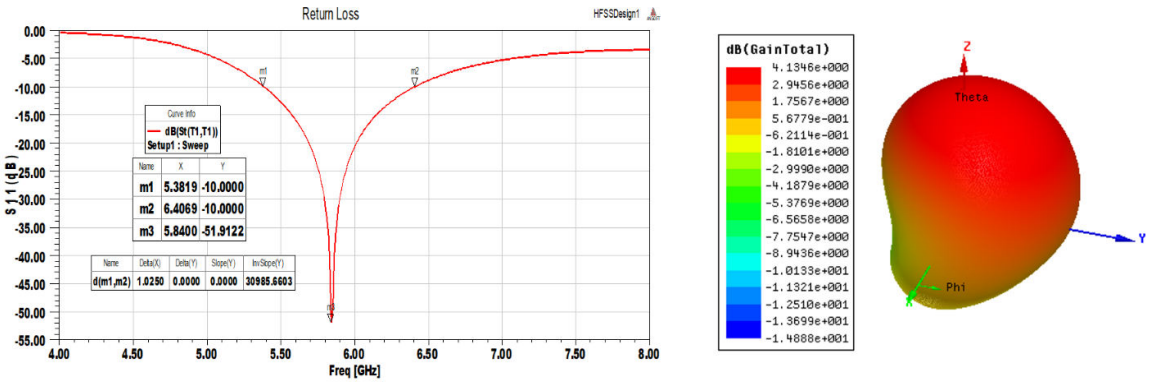

Figure-2. Return Loss and 3D-Total gain in dB for the proposed antenna.

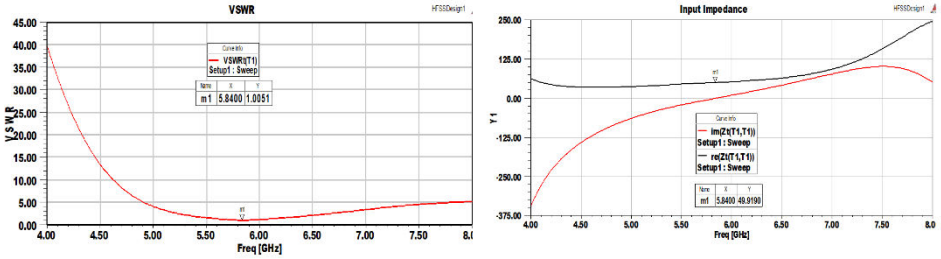

Figure-3. VSWR and Input Impedance for the proposed antenna.

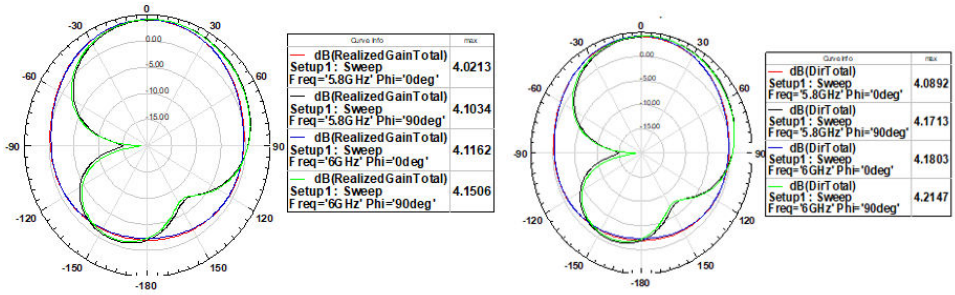

Figure-4. 2D-Total gain and 2D-Total Directivity in dB for the proposed antenna.

After finalizing the theoretical design of the semicircular Planar Inverted-F Antenna (PIFA) using HFSS simulation software, the antenna was physically built in the Antennas Laboratory at the University of Basrah, as shown in Figure-5.

Figure-5. The prototype proposed a PIFA antenna.

To evaluate its real-world performance, the reflection coefficient (S_{11}) was measured using a Vector Network Analyzer (PLANAR 804/1), and the results were compared to the simulated data to verify the accuracy of the design.

As shown in Figure-6, there is a comparison between the simulated and measured S_{11} responses. The simulation showed a minimum S_{11} of -51.9 dB at a resonant frequency of 5.84 GHz, indicating excellent impedance matching. In the experimental measurement, the lowest S_{11} value reached -36.8 dB at the same frequency, which still represents strong performance.

Regarding bandwidth, the simulation predicted a -10 dB bandwidth ranging from 5.38 GHz to 6.40 GHz, giving an overall span of about 1.02 GHz. In contrast, the measured -10 dB bandwidth extended from 5.48 GHz to 6.30 GHz, resulting in a bandwidth of roughly 0.82 GHz.

The minor differences often observed between theoretical predictions and experimental results in antenna design can be attributed to several factors. These include simplified assumptions used in theoretical models, slight inaccuracies during fabrication, imperfect soldering, and variations in the actual material properties compared to those assumed. Additionally, environmental conditions and the limitations of measurement equipment can influence the results.

Overall, the strong alignment between the simulated and measured results supports the effectiveness of the antenna design and demonstrates its potential for use in practical C-band wireless communication systems.

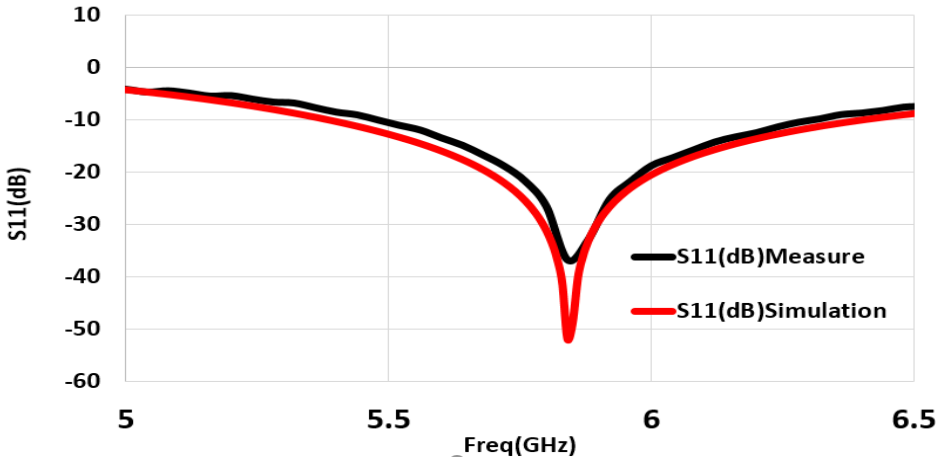

Figure-6. Simulation and measured results of the proposed PIFA semicircular antenna.

3.1 MIMO Antenna

After designing the single antenna, its key performance parameters were evaluated, including the loss factor, radiation characteristics, gain, directivity, and input impedance. Based on these findings, the next phase focuses on developing a two-element MIMO (Multiple-Input Multiple-Output) antenna array. The performance of this MIMO system will be assessed by calculating its loss factor and analyzing the mutual coupling between the two antenna elements. As shown in Figure-7, the top and bottom of the proposed MIMO array consist of two antennas. Studying mutual coupling is essential, as it affects both the efficiency and isolation of the MIMO system. By optimizing the spacing between elements and minimizing coupling effects, the overall performance of the system can be improved, making it more suitable for high-speed wireless communication applications.

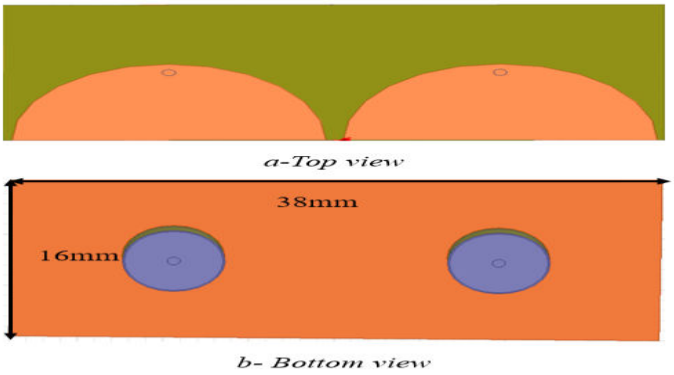

Figure-7. Top and bottom view for the position of MIMO antennas.

Figure-8 presents the return loss and mutual coupling between the two elements in the MIMO array. The results show that the array maintained the almost same resonant frequency range as the single antenna while achieving a bandwidth of 0.66GHz. Additionally, the mutual coupling was measured at -19.46 dB at 5.85 GHz. Preserving the resonant frequency ensures that the MIMO configuration does not alter the operational characteristics of the individual antenna elements. Moreover, the observed mutual coupling remains within an acceptable range, indicating good isolation between the elements. This is crucial for reducing interference and optimizing the overall performance of the MIMO system.

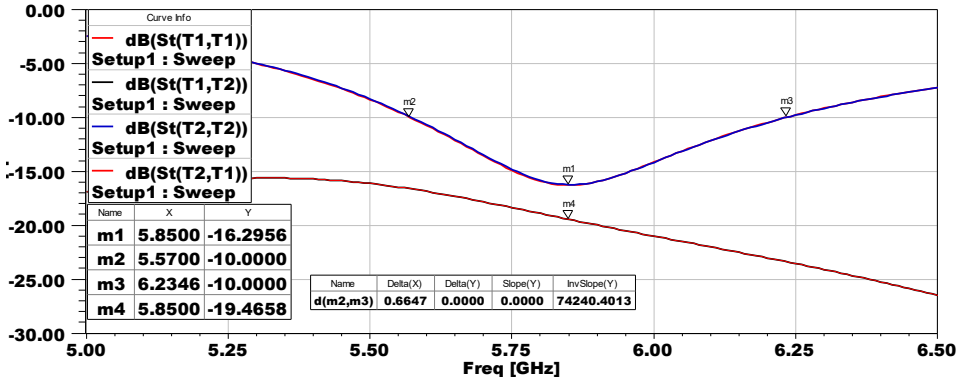

Figure-8. Return loss and mutual coupling for the first configuration.

Figure-9 illustrates the radiation pattern, showing the directivity and gain distributions in the E and H planes. The highest directivity value was recorded at 6.4dB. Figure-10 illustrates the gain in three dimensions, with the highest gain value reaching 6.15dB at 5.8GHz This is a significant increase compared to a single antenna, and reflects the effect of the array in enhancing radiation performance.

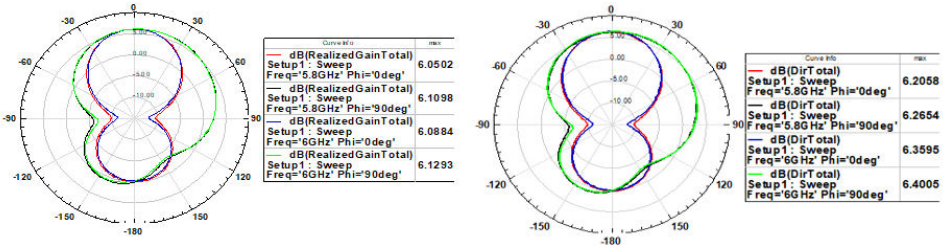

Figure-9. 2D-Total gain and 2D-Total Directivity in dB.

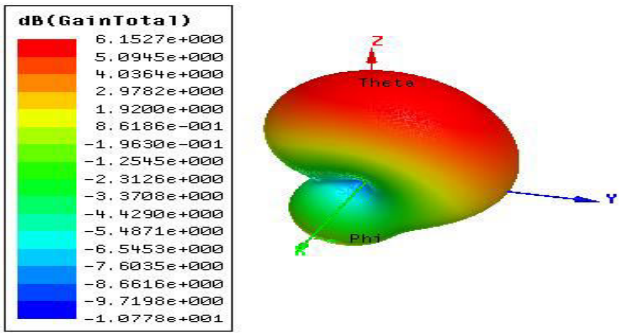

Figure-10. 3D-Total gain in dB.

After completing the HFSS simulation of the two-element MIMO PIFA array, the design was brought to life through fabrication, as shown in Figure-11. To evaluate how well the antenna performed in practice, key S-parameters were measured and analyzed.

Figure-11. Prototype of the proposed MIMO antenna.

Figure-12 shows the measured S-parameters of the fabricated PIFA array. A slight difference was observed between the return loss of Antenna 1 (S_{11}) and Antenna 2, which is likely due to small inconsistencies during the fabrication process, such as uneven soldering or subtle structural variations. These types of variations are common in hardware prototypes and can cause minor differences between antenna elements.

The mutual coupling, indicated by S_{21}, dropped to -32.7 dB at the resonance frequency of 5.85 GHz, suggesting excellent isolation between the two antennas a critical factor for effective MIMO system performance.

Additionally, the proposed design demonstrated significantly lower mutual coupling across the entire operating frequency band when compared to typical two-element PIFA arrays placed on a conventional ground plane. This improvement confirms that the design successfully reduces interference between the antenna elements, enhancing the overall performance of the MIMO configuration.

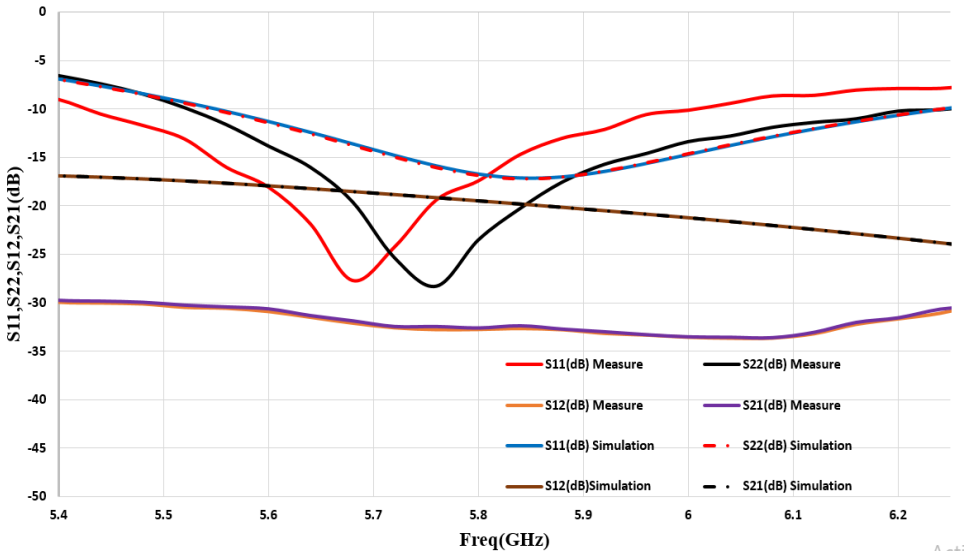

Figure-12. Simulated and measurement results of return loss, coupling, and transmitting coefficients for the MIMO antenna.

3.2 Defected Ground Structure (DGS)

To reduce the mutual coupling between two antennas in a MIMO array, a simple modification was made by adding two rectangular slots to the ground plane. These slots were positioned exactly midway between the two antenna elements. Each slot has dimensions of 2.225 mm in length and 1 mm in width, as shown in Figure-13. Simulation results, illustrated in Figure-14, show that this approach significantly improved isolation, with the mutual coupling (S21) dropping from -19.46 dB to -40.71 dB after introducing the slots.

Besides reducing coupling, this structural change also led to an improvement in the antenna's bandwidth. The -10 dB impedance bandwidth expanded to cover the range from 5.43 GHz to 6.21 GHz, whereas the original design supported a narrower range from 5.57 GHz to 6.23 GHz. This indicates that the antenna can now operate more effectively over a wider frequency range.

Improved isolation between antenna elements is especially important in MIMO systems, as it helps maintain signal clarity and reduces interference. As a result, key system performance factors such as channel capacity, diversity gain, and overall efficiency are positively impacted. Therefore, reducing mutual coupling is a critical aspect of antenna design in modern high-performance MIMO communication systems.

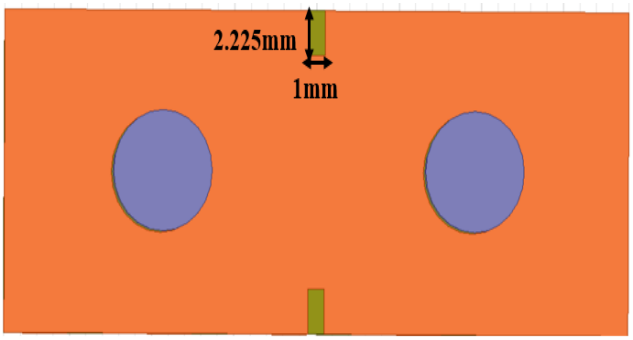

Figure-13. Configurations of slits on the ground plane.

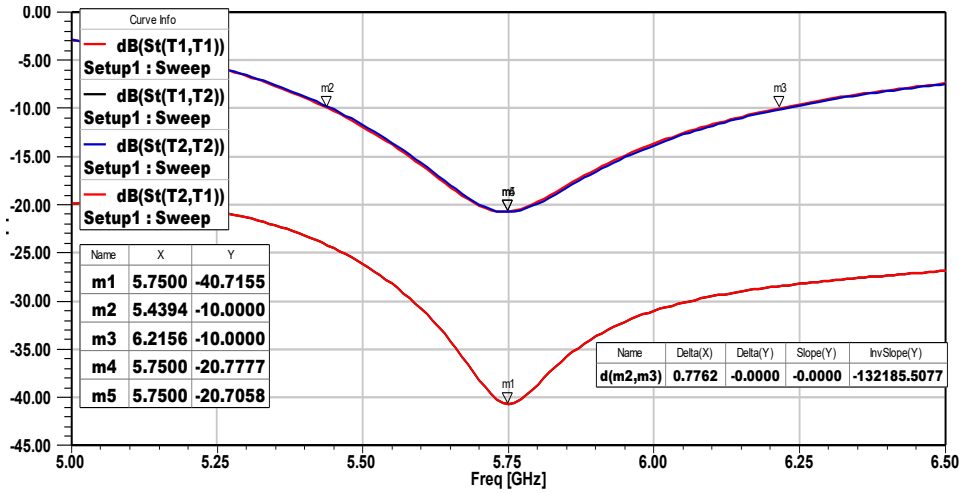

Figure-14. Return loss and mutual coupling for the modifiedfirst configuration.

Figure-15 illustrates the radiation pattern, showing the directivity and gain distributions in the E and H planes. The highest directivity value was recorded at 6.46dB. Figure-16 illustrates the gain in three dimensions, with the highest gain value reaching 6.25dB. We notice from Figures 15 and 16 a slight improvement in directionality and achievement.

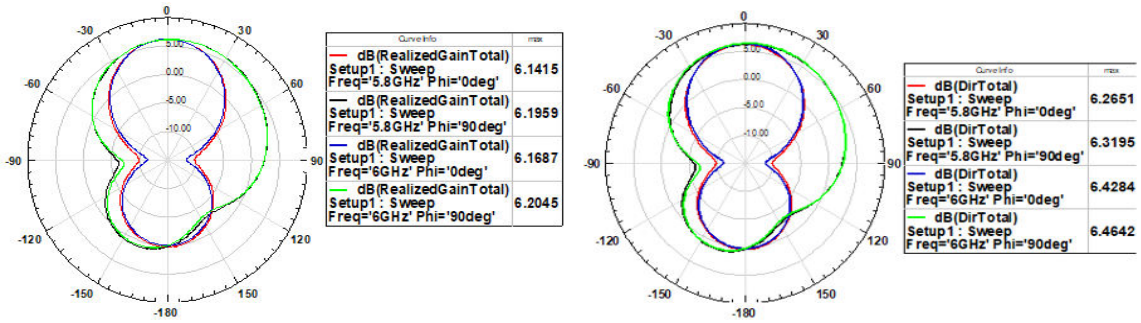

Figure-15. 2D-Total gain and 2D-Total Directivity in dB for the modified ground plan antenna.

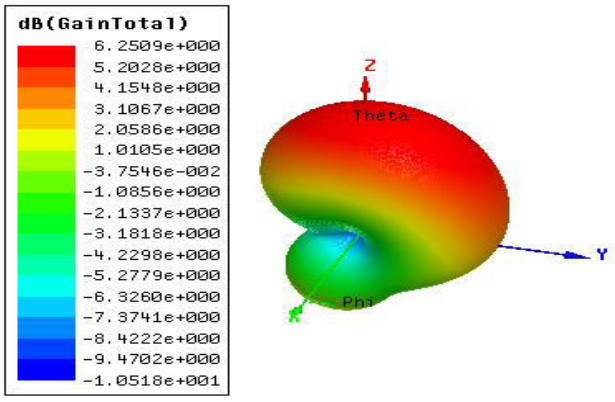

Figure-16. 3D-Total gain in dB.

A two-element PIFA antenna array was successfully fabricated, incorporating the designed ground slots as shown in Figure-17. To evaluate the antenna's real-world performance, key S-parameters were measured.

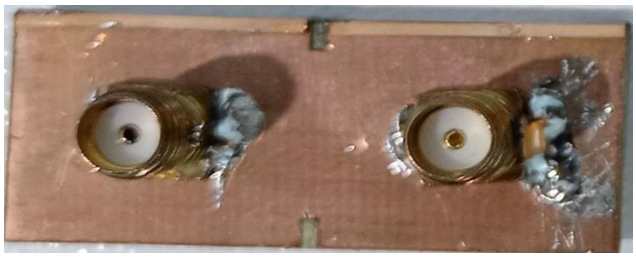

Figure-17. Manufacturing proposed MIMO antenna

The measured results are displayed in Figure-18. A slight difference was noted between the return losses of Antenna 1 (S_{11}) and Antenna 2 (S_{22}), most likely caused by minor inconsistencies during fabrication. Such small variations are typical in physical prototypes and can result in subtle performance differences between antenna elements.

At the resonant frequency of 5.75 GHz, the mutual coupling (S21) was measured at -35.4 dB. Although this is slightly higher than the simulated result of -40.7 dB at the same frequency, the measured value still indicates a high

level of isolation between the two antennas, an essential factor for the efficient functioning of MIMO systems. The close alignment between the measured and simulated data confirms the reliability of the design and the precision of the fabrication process.

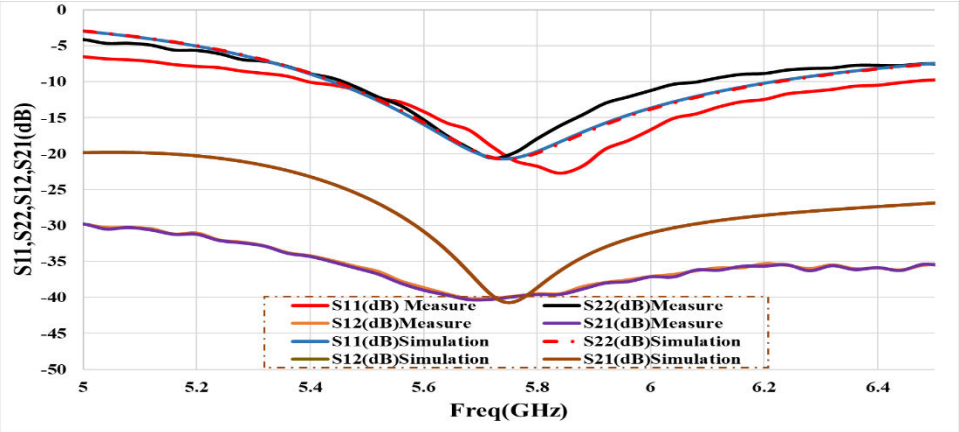

Figure-18. Simulated and measurement results of return loss, coupling, and transmitting coefficients for the modified MIMO antenna.

Across the entire operating frequency range, the antenna array consistently demonstrated lower mutual coupling compared to typical two-element PIFA arrays with standard ground planes. This performance boost clearly shows that adding ground slots helps reduce electromagnetic interaction between the antennas, improving signal clarity and reducing interference. These enhancements in isolation and bandwidth make the proposed antenna design a strong candidate for high-efficiency MIMO systems in modern wireless communications.

A dual-element MIMO antenna array was designed and initially assessed through full-wave simulations using Ansys HFSS. Key parameters such as return loss (S_{11}), mutual coupling (S_{21}), gain, and directivity were analyzed. Following the simulation, a physical prototype of the antenna array was fabricated. The measured S-parameters from the prototype closely matched the simulated values, confirming both the accuracy of the design and the success of the fabrication process.

3.2.1 MIMO performance metrics

To further assess the practical performance of the MIMO array in real-world wireless communication scenarios, several critical metrics were examined. These included the:

• Envelope Correlation Coefficient (ECC): Calculated from S-parameters using [27]:

$$ECC = \frac{|S_{11}^{*}S_{12}+S_{21}^{*}S_{22}|^2}{(1-(|S_{11}|^2+|S_{21}|^2))(1-(|S_{21}|^2+|S_{12}|^2))} \quad \ldots\ldots\ldots\ldots 3$$

As shown in Figure-19, the ECC value at the target frequency of 5.75 GHz was approximately 0.0, which is well below the recommended maximum of 0.5. This indicates excellent isolation and low correlation between the antenna elements, ideal for effective MIMO operation.

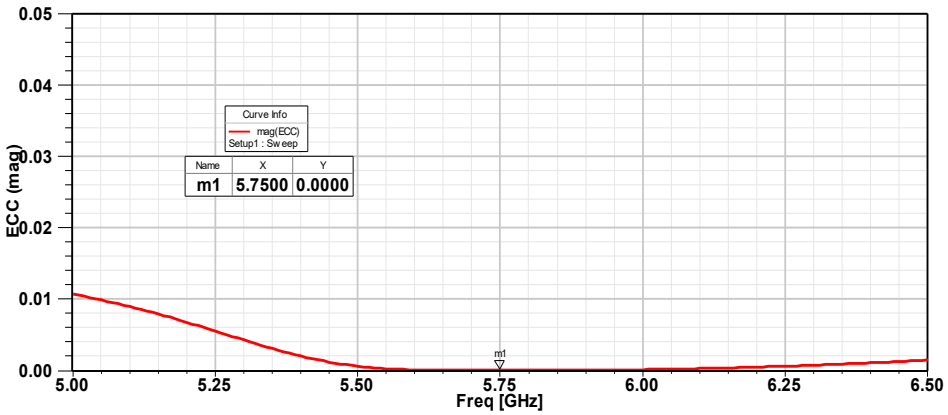

Figure-19. Simulated ECC of the suggested modified MIMO antenna.

• Diversity Gain (DG): Defined as [28]:

$$DG = 10 \times \sqrt{1 - |ECC|^2} \quad \ldots\ldots\ldots\ldots\ldots\ldots\ldots\ldots\ldots\ldots 4$$

Figure-20 shows that the Diversity Gain reached 10 dB at 5.75 GHz, which matches the ideal value and reflects strong diversity performance.

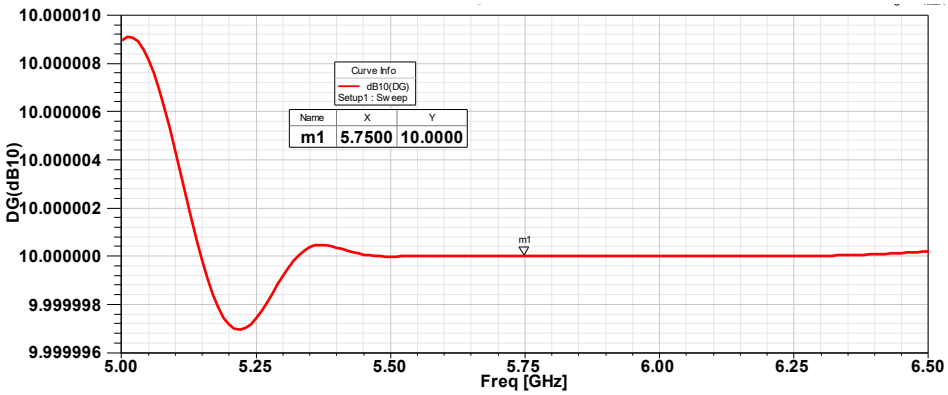

Figure-20. Simulated DG of the suggested modified MIMO antenna.

• Channel Capacity Loss (CCL): Given by [29]:

$$\mathrm{CCL} = -\log_2 \det(\psi R) \quad \ldots\ldots\ldots\ldots\ldots\ldots\ldots\ldots\ldots\ldots 5$$

Channel Capacity Loss (CCL), illustrated in Figure-21, was found to be just 0.0085 bits/s/Hz at 5.75 GHz. This value is far below the upper limit of 0.4 bits/s/Hz, confirming that the antenna array introduces minimal capacity degradation due to coupling or pattern correlation.

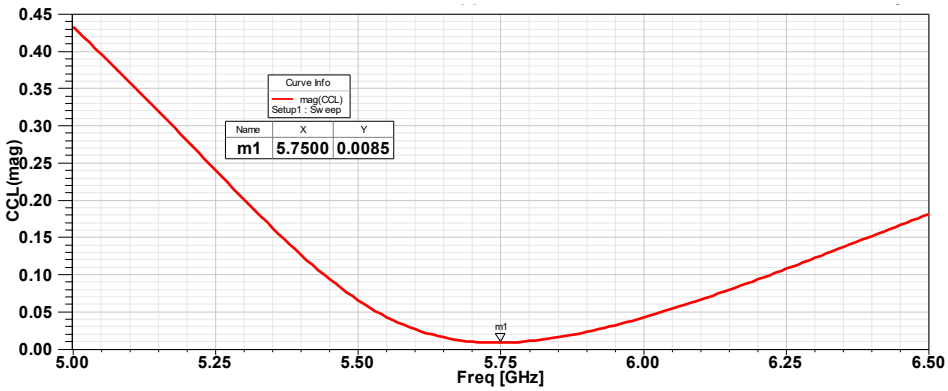

Figure-21. Simulated CCL of the suggested modified MIMO antenna.

• Mean Effective Gain (MEG): Defined as [29]:

$$MEG = \frac{\left[1-|S_{ii}|^2+|S_{ij}|^2\right]}{\left[1-|S_{ij}|^2+|S_{jj}|^2\right]} \quad \ldots\ldots\ldots\ldots\ldots\ldots\ldots\ldots\ldots\ldots 6$$

The Mean Effective Gain (MEG), displayed in Figure-22, was measured at −0.0038 dB. This is within the acceptable range of ±3 dB, indicating a balanced reception performance between antenna elements.

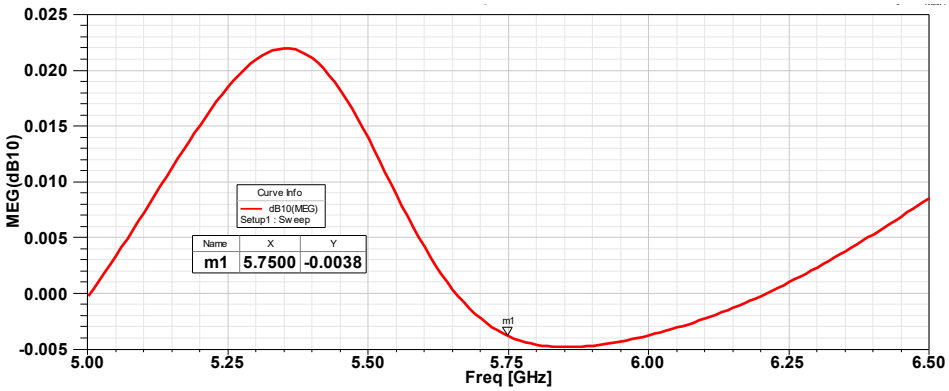

Figure-22. Simulated MEG of the suggested modified MIMO antenna.

• Total Active Reflection Coefficient (TARC): Defined as [30].

$$TARC = \frac{\sqrt{(|(S_{11}+S_{12}e^{j\theta})|^2+(|(S_{21}+S_{22}e^{j\theta})|^2)}}{\sqrt{2}} \quad \ldots\ldots\ldots\ldots 7$$

At 5.75 GHz, TARC reached −33.4 dB as seen in Figure-23, confirming excellent impedance matching under multi-port excitation. These metrics collectively demonstrate the antenna's suitability for practical MIMO applications.

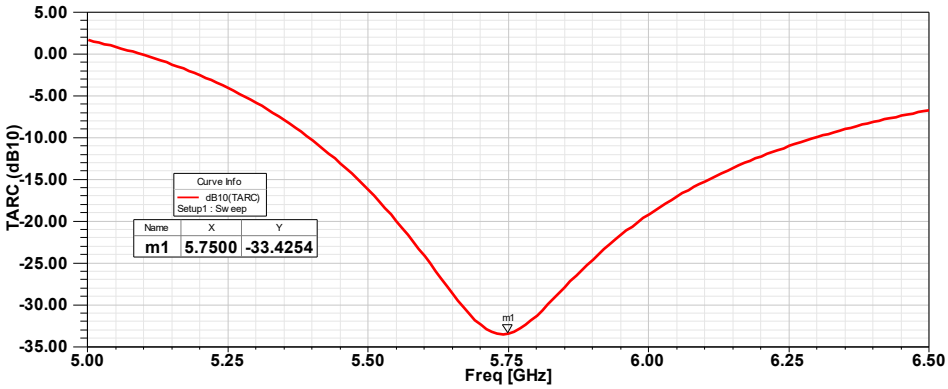

Figure-23. Simulated TARC of the suggested modified MIMO antenna.

4. CONCLUSIONS

In this work, a compact semicircular PIFA MIMO antenna with slotted ground plane modifications was designed, simulated, and experimentally validated. The introduction of simple rectangular slots in the ground plane significantly reduced mutual coupling from −19.46 dB to −40.71 dB in simulation and −35.4 dB in measurement. The design achieved excellent ECC, DG, CCL, MEG, and TARC performance, confirming its effectiveness in enhancing diversity and capacity. Compared to recent literature, the proposed design offers higher isolation in a much smaller footprint. These attributes make the antenna a strong candidate for next-generation compact wireless systems, particularly for C-band 5G, Wi-Fi, and IoT devices.

ACKNOWLEDGMENTS

The authors gratefully acknowledge support from the Department of Physics, College of Science, University of Basra, Iraq.

REFERENCES

[1] R. Malallah, R. M. Shaaban, and A. Wa'il. 2020. A dual-band star-shaped fractal slot antenna: Design and measurement. AEU-International Journal of Electronics and Communications. 127: 153473.

[2] S. S. Al-Bawri *et al*. 2021. Broadband Sub-6GHz Slot-based MIMO antenna for 5G NR bands mobile applications. in Journal of Physics: Conference Series. 1962(1): 12038.

[3] S. Hameed, H. A. Yasser, and A. H. Al-Shaheen. 2025. Microstrip Patch Antenna Array Design and Mutual Coupling Reduction for Wi-Fi and Wi-Max Applications. University of Thi-Qar Journal of Science. 12(1): 30-35.

[4] M. K. Ibraheem and H. M. AlSabbagh. 2013. A comparison study for channel capacity of MIMO systems with Nakagami-M., Weibull, and Rice distributions. International Journal of Science and Engineering Investigations.

[5] H. Q. Al-fayyadh, H. M. AlSabbagh, and H. Al-Rizzo. 2017. Flexible Compact Mimo T-Shape Antenna with Bridge Square Split-Ring Resonator. J. Model. Simul. Antennas Propag. pp. 1-7.

[6] J. Winters. 1987. on the capacity of radio communication systems with diversity in a Rayleigh fading environment. IEEE journal on selected areas in communications. 5(5): 871-878.

[7] G. J. Foschini. 1996. Layered space-time architecture for wireless communication in a fading environment when using multi-element antennas. Bell Labs Technical Journal. 1(2): 41-59.

[8] E. Telatar. 1999. Capacity of multi-antenna Gaussian channels. European transactions on telecommunications. 10(6): 585-595.

[9] Warren L. Stutzman, Gary A. Thiele, Antenna Theory and Design-Wiley (2012) _2.pdf.

[10] P. N. Fletcher, M. Dean, and A. R. Nix. 2003. Mutual coupling in multi-element array antennas and its influence on MIMO channel capacity. Electronics Letters. 39(4): 342-344.

[11] E. Skafidas and R. J. Evans. 2004. Antenna effects on the capacity of MIMO communications systems in Rayleigh channels. In 2004 IEEE 15th International Symposium on Personal, Indoor and Mobile Radio Communications (IEEE Cat. No. 04TH8754). 1: 617-621.

[12] D. P. McNamara, M. A. Beach, and P. N. Fletcher. 2001. Experimental investigation into the impact of mutual coupling on MIMO communication systems. In 4th International Symposium on Wireless Personal Multimedia Communications (WPMC 2001), Aalborg, Denmark.

[13] C. Borja, A. Algans, M. Royo, J. Anguera and C. Puente. 2003. Impact of the antenna technology and the antenna parameters on the performance of MIMO systems. In the IEEE Antennas and Propagation Society International Symposium. Digest. Held in conjunction with: USNC/CNC/URSI North American Radio Sci. Meeting (Cat. No. 03CH37450). 2: 507-510.

[14] Y. Gao, X. Chen, Z. Ying, and C. Parini. 2007. Design and performance investigation of a dual-element PIFA array at 2.5 GHz for MIMO terminal. IEEE Transactions on Antennas and Propagation. 55(12): 3433-3441.

[15] C. C. Chiau, X. Chen, and C. G. Parini. 2005. A miniature dielectric-loaded folded half-loop antenna and ground plane effects. IEEE antennas and wireless propagation letters. 4: 459-462.

[16] Y. Gao, C. C. Chiau, X. Chen, and C. G. Parini. 2005. Modified PIFA and its array for MIMO terminals. IEE Proceedings-Microwaves, Antennas and Propagation. 152(4): 255-259.

[17] X. Xiong, W. LI, X. TAN and Y. HU. 2025. Mutual Coupling Reduction for Dual-Band MIMO Antenna via Artificial Transmission Line. IEICE Transactions on Electronics. 108(1): 16-23.

[18] R. Mäkinen, V. Pynttäri, J. Heikkinen and M. Kivikoski. 2007. Improvement of antenna isolation in hand-held devices using miniaturized electromagnetic band-gap structures. Microwave and Optical Technology Letters. 49(10): 2508-2513.

[19] F. Yang and Y. Rahmat-Samii. 2003. Microstrip antennas integrated with electromagnetic band-gap (EBG) structures: A low mutual coupling design for array applications. IEEE transactions on antennas and propagation. 51(10): 2936-2946.

[20] C. C. Chiau, X. Chen, and C. G. Parini. 2005. A sandwiched multiperiod EBG structure for microstrip patch antennas. Microwave and Optical Technology Letters. 46(5): 437-440.

[21] X. Tan, W. Wang, Y. Wu, Y. Liu and A. A. Kishk. 2019. Enhancing isolation in dual-band meander-line multiple antenna by employing a split EBG structure. IEEE Transactions on Antennas and Propagation. 67(4): 2769-2774.

[22] M. S. Sharawi, A. B. Numan, M. U. Khan, and D. N. Aloi. 2012. A dual-element dual-band MIMO antenna system with enhanced isolation for mobile terminals. IEEE antennas and wireless propagation letters. 11: 1006-1009.

[23] Karaboikis, Soras, Tsachtsiris and Makios. 2004. Compact dual-printed inverted-F antenna diversity systems for portable wireless devices. IEEE antennas and wireless propagation letters. 3: 9-14.

[24] C.-Y. Chiu, C.-H. Cheng, R. D. Murch, and C. R. Rowell. 2007. Reduction of mutual coupling between closely-packed antenna elements. IEEE transactions on antennas and propagation. 55(6): 1732-1738.

[25] W. Wang, Y. Wu, W. Wang and Y. Yang. 2020. Isolation enhancement in dual-band monopole antenna for 5G applications. IEEE Transactions on Circuits and Systems II: Express Briefs. 68(6): 1867-1871.

[26] D. H. Hashim. 2023. Design and Simulation of Arrays of Modified Circular Microstrip Antenna Excited by Two Orthogonal Feeders and Two Dielectric Substrates. University of Basrah.

[27] J. Thaysen and K. B. Jakobsen. 2006. Envelope correlation in (N, N) MIMO antenna array from scattering parameters. Microwave and Optical Technology Letters. 48(5): 832-834.

[28] P. Garg, P. Jain. 2020. Isolation improvement of MIMO antenna using a novel flower-shaped metamaterial absorber at 5.5GHz WiMAX band. IEEE Trans. Circuits Syst. pp. 675-679.

[29] M. Khalid et al. 2020. 4-port MIMO antenna with defected ground structure for 5G millimeter wave applications. Electronics (Switzerland). 9(1).

[30] P. Sharma, R. N. Tiwari, P. Singh, P. Kumar, and B. K. Kanaujia. 2022. MIMO antennas: Design approaches, techniques and applications. Sensors. 22(20): 7813.